

Advanced Synthetic Aperture Radar Imaging and Feature Analysis^{*}

Victor C. Chen, Ronald Lipps, Maitland Bottoms
Radar Division, Naval Research Laboratory, Washington D.C., U.S.A.

Abstract—In this paper, we review and discuss advanced algorithms for synthetic aperture radar image formation, the effect of motion perturbation on radar imaging, synthetic aperture radar imaging of ground moving targets, and micro-Doppler feature analysis.

Key Words: Synthetic aperture radar, image formation, ISAR imaging, SAR GMTI, radar micro-Doppler

I. INTRODUCTION

Synthetic aperture radar (SAR) generates a range and cross-range image when radar is moving. Inverse synthetic aperture radar (ISAR) is a variation of the SAR that generates a range-Doppler image of targets by coherently processing radar returns at different target aspect angle due to relative motions between the radar and the target [1].

The distribution of radar reflectivity over a target can be measured through the Doppler spectrum at each range bin by taking the Fourier transform over the phase history time series. If the motion or rotations are accompanied by perturbations, the phase of the returned signal becomes non-linear. Thus, the image of the target may be degraded when using the conventional imaging algorithms. Recent efforts in ISAR polar reformatting, super-resolution spectral analysis and time-frequency based image formation offer improvements in radar imagery over the commonly used Fourier transform approach. Study of the effect of motion perturbations on ISAR imaging is important. In this paper, commercial small craft accompanying with the GPS information is used to study this effect.

For SAR, if there are moving objects in the scene, it cannot simultaneously produce clear images of stationary objects as well as moving objects. The moving object appears as defocused and spatially displaced one superimposed on the SAR scene. The important issue is how to detect and focus images of a moving target in SAR. Moreover, because of the additional Doppler caused by target's motion, the detected and focused target may not be located in its true location in the SAR scene. Many algorithms have been proposed to re-locate the detected target to its true location: some uses a single channel antenna and some uses multiple antennas.

Micro-motion dynamics of a target or structures on the target may induce frequency modulations on the returned signal and generate side-bands about the target's Doppler frequency shift, called the micro-Doppler effect. This effect enables us to determine some properties of targets.

This paper is a review of advanced radar image formation algorithms, the effect of motion perturbations on radar imaging, SAR imaging of ground moving targets, and micro-Doppler in radar.

II. RADAR IMAGE FORMATION AND SUPER-RESOLUTION

The basic algorithm for a SAR/ISAR image formation is the range-Doppler processing [2]. Modern motion compensation techniques can provide good focus for a limited number of scatterers on the target. To achieve a fully focused ISAR image, the problems dealing with target rotation and scatterers' migration through range cells need to be addressed. ISAR Polar reformatting was proposed for this purpose.

The common method for Doppler processing is the Fourier transform. For short data sets, where the Fourier processing has bias in frequency estimate and a loss of precision, super-resolution approaches can be used to enhance the Doppler resolution. Further more, when Doppler spectrum becomes time-varying, a time-frequency based image formation may be used to replace Fourier method and generates clear images of targets.

A. ISAR Polar Reformatting

Polar reformatting is an image formation technique based on tomography. It involves reconstructing the spatial representation of an object by applying the Fourier transform to a set of observations, each being a projection of the object onto a line, taken over a series of aspect angles. This series of observations populates a region of Fourier space and can be used to reconstruct an image of the object by applying inverse Fourier transforms.

Polar reformatting techniques have been developed in spotlight SAR imaging [3] and has been adapted for use in ISAR imaging [4]. A received radar pulse is the projection

^{*} This work was sponsored by the ONR 313 Direct and ONR Base at NRL.

Report Documentation Page				Form Approved OMB No. 0704-0188	
Public reporting burden for the collection of information is estimated to average 1 hour per response, including the time for reviewing instructions, searching existing data sources, gathering and maintaining the data needed, and completing and reviewing the collection of information. Send comments regarding this burden estimate or any other aspect of this collection of information, including suggestions for reducing this burden, to Washington Headquarters Services, Directorate for Information Operations and Reports, 1215 Jefferson Davis Highway, Suite 1204, Arlington VA 22202-4302. Respondents should be aware that notwithstanding any other provision of law, no person shall be subject to a penalty for failing to comply with a collection of information if it does not display a currently valid OMB control number.					
1. REPORT DATE 14 APR 2005		2. REPORT TYPE N/A		3. DATES COVERED -	
4. TITLE AND SUBTITLE Advanced Synthetic Aperture Radar Imaging and Feature Analysis				5a. CONTRACT NUMBER	
				5b. GRANT NUMBER	
				5c. PROGRAM ELEMENT NUMBER	
6. AUTHOR(S)				5d. PROJECT NUMBER	
				5e. TASK NUMBER	
				5f. WORK UNIT NUMBER	
7. PERFORMING ORGANIZATION NAME(S) AND ADDRESS(ES) Radar Division, Naval Research Laboratory, Washington D.C.,U.S.A.				8. PERFORMING ORGANIZATION REPORT NUMBER	
9. SPONSORING/MONITORING AGENCY NAME(S) AND ADDRESS(ES)				10. SPONSOR/MONITOR'S ACRONYM(S)	
				11. SPONSOR/MONITOR'S REPORT NUMBER(S)	
12. DISTRIBUTION/AVAILABILITY STATEMENT Approved for public release, distribution unlimited					
13. SUPPLEMENTARY NOTES See also ADM001798, Proceedings of the International Conference on Radar (RADAR 2003) Held in Adelaide, Australia on 3-5 September 2003., The original document contains color images.					
14. ABSTRACT					
15. SUBJECT TERMS					
16. SECURITY CLASSIFICATION OF:			17. LIMITATION OF ABSTRACT UU	18. NUMBER OF PAGES 8	19a. NAME OF RESPONSIBLE PERSON
a. REPORT unclassified	b. ABSTRACT unclassified	c. THIS PAGE unclassified			

of the electromagnetic scattering from the target onto the radar line-of-sight (LOS) and can be used for this technique. The difference between tomographic reconstruction using radar signals and traditional tomographic reconstruction is that the radar's signal is modulated by the carrier frequency. As a result, the Fourier transform of the radar pulse produces a line segment in the 3-D Fourier space that is offset from the origin by the carrier frequency at an angle determined by the angle of the radar LOS. As successive pulses are received and the aspect between the radar and the target changes, the line segment sweeps out a data surface in 3-D Fourier space as shown in Figure 1. Once the data surface is formed, an image is reconstructed by transforming the surface into the spatial domain using a variety of techniques developed for SAR.

The polar reformatting process for ISAR imaging is similar to that for spotlight SAR imaging. The main difference is that in ISAR processing the motion of the target provides the change in aspect necessary for Doppler processing, whereas in spotlight SAR the change in aspect comes from the motion of the radar. As a consequence of this difference, the aspect change between the radar and the

target is both unknown and uncontrollable in the ISAR imaging. Because the aspect change defines the shape of the data surface, the rotation of the target must be determined before polar reformatting can be used to process the data into imagery. Instead of modeling the target motion, we model the data surface directly and use measurable scatterer motion quantities, such as range, Doppler and translation acceleration, to estimate the data surface model parameters. We chose a quadratic data surface model that uses fewest parameters but still allowed us to compensate for the majority of non-linear rotational motion in the target. Within the surface, the spacing between the data line segments is also modeled as a quadratic function. In this model, there are two parameters of interest: the quadratic term representing the curvature of the data surface, called the out-of-plane acceleration, and the quadratic term representing the line segment spacing, called the in-plane acceleration.

The implementation of this technique involves measuring the target motion from the data, estimating parameters for the data surface model, projecting the data surface onto a planar surface, re-interpolating the data into equally spaced samples, and performing the inverse

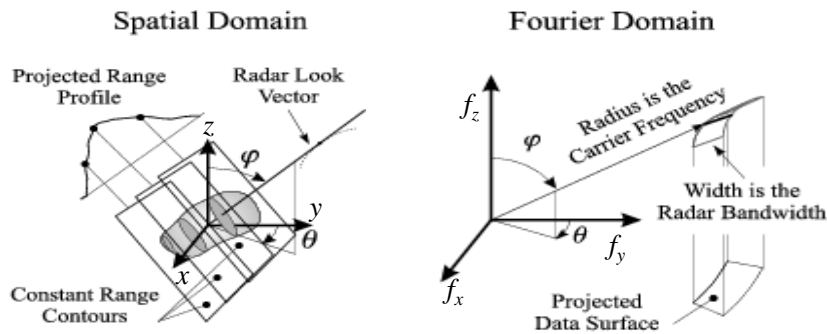


Figure 1 Representation of the received radar pulses for a rotating target in the spatial and Fourier domains.

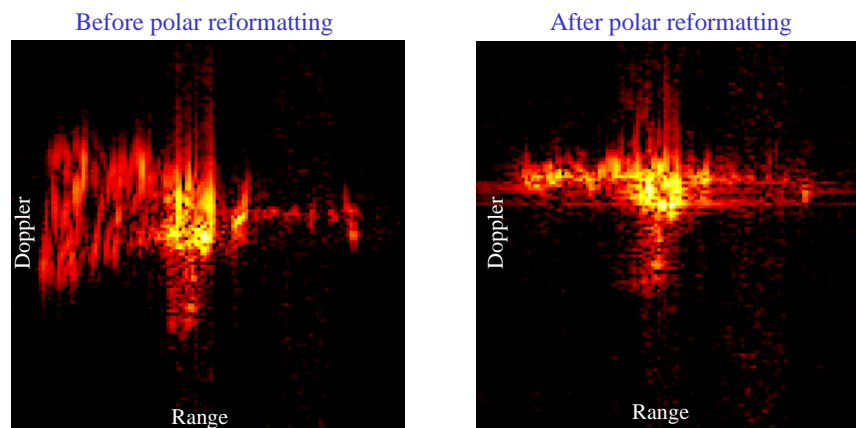


Figure 2. Examples ISAR imagery of a ship showing the improvement in image quality using polar reformatting.

Fourier Transform. Figure 2 shows the comparison of imagery produced by the conventional and the polar reformatting method and the improvement in the image quality can be seen. Polar reformatting can produce high quality imagery even in conditions with significantly complex target motion.

B. Modern Spectral Estimation

Since the motion dynamic of the target is unknown, using longer observation time is not desirable. Problems with small data sets using the Fourier transform are bias in the estimate and a loss of precision due to the spoiling of the instantaneous frequency with the convolution by the broadness of the imposed window function. However, as the observation interval shrinks the assumption that the Doppler frequency of the scatterers does not change during the observation becomes more valid.

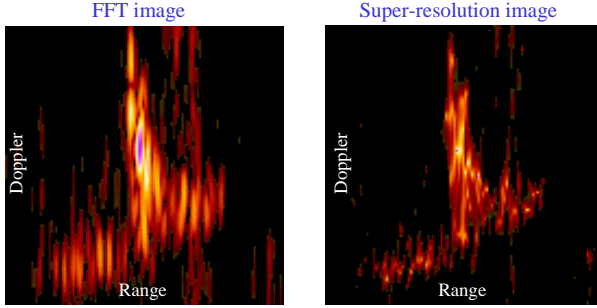


Figure 3 FFT vs. AR Doppler image.

At a given instant, radar return from a point scatterer will have a single phase delay and frequency offset, depending upon its range and instantaneous LOS velocity respectively. Such a signal, a sinusoid in noise, can be modeled as an auto-regressive process, and there are useful relationships between AR processes and their spectra. Marple [5] expands upon the variety of approaches

exploiting these characteristics. His modified covariance spectral estimation technique has yielded excellent results for ISAR imaging. The localization and sharpening is called super-resolution. Figure 3 illustrates the more tightly resolved Doppler characteristic of super-resolution images compared to FFT images [6]. Super-resolution radar imaging using modern spectral estimation can also be found in [7-10].

C. Time-Frequency Based Image Formation

The conventional radar imaging system is based on the Fourier transform and assumes that Doppler shifts are constant. However, when Doppler spectrum is time-varying, Fourier based images become blurred and time-frequency transforms should be used to generate clear images of moving targets [11-13].

Figure 4 illustrates the time-frequency based radar imaging system. The standard motion compensation is used prior to the time-frequency image formation. The Fourier-based image formation generates only one image frame from an $M \times N$ I/Q data. The data consists of M time history series, each having length of N . However, the time-frequency based image formation takes the time-frequency transform for each time history series and generates an $N \times N$ time-Doppler distribution. By combining the M time-Doppler distributions at M range cells, the $N \times M \times N$ time-range-Doppler cube $Q(r_m, f_n, t_n)$ can be formed as

$$Q(r_m, f_n, t_n) = TF\{G(r_m(n))\}$$

where TF denotes the time-frequency operation with respect to the variable n .

At a particular time instant t_i , only one range-Doppler image frame $Q(r_m, f_n, t_n = t_i)$ can be extracted from the cube. There are a total of N image frames available, and every one represents a full range-Doppler image at a particular time instant. Therefore, by replacing the Fourier transform with the time-frequency transform, a 2-D range-Doppler Fourier image frame becomes a 3-D time-range-

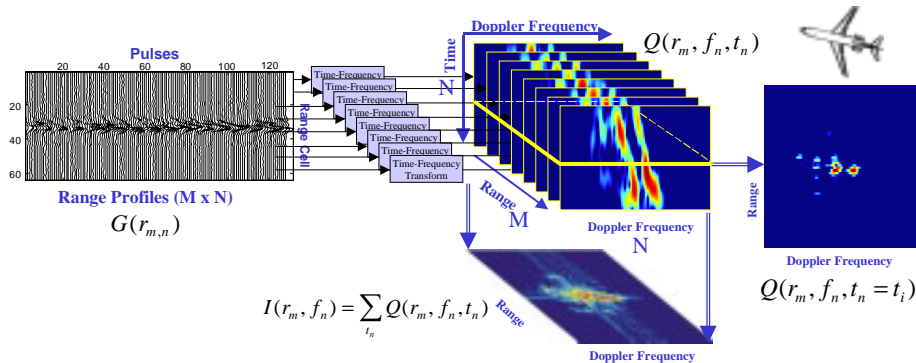


Figure 4. Block diagram of time-frequency based image formation.

Doppler image cube. The integration of the N time frames is the Fourier image. By sampling the image cube in time, a time sequence of 2-D range-Doppler images can be viewed. Each individual time-sampled frame from the cube provides not only a clear image with superior resolution but also time-varying properties from one time to another as shown in Figure 5.

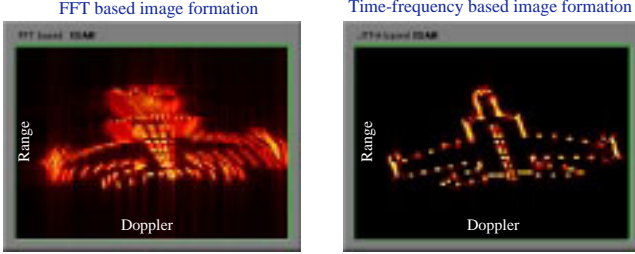


Figure 5. Comparison of FFT based image and time-frequency based image.

III. THE EFFECT OF MOTION PERTURBATIONS ON ISAR IMAGING

A target can be considered as a rigid body with 6 degrees of freedom: three translations along x, y, z directions, and three rotations – roll, pitch and yaw. The roll, pitch, and yaw motions are described by a rotation matrix $\mathfrak{R}(\theta_r, \theta_p, \theta_y)$, which is a function of the roll angle θ_r , pitch angle θ_p , and yaw angle θ_y . The instantaneous position vector \vec{r} of a scatterer at time t is determined by its previous position \vec{r}_0 at time t_0 and the rotation matrix. The Doppler shift is [14]

$$f_D = \frac{2f_c}{c} \frac{d\mathfrak{R}(\theta_r, \theta_p, \theta_y)}{dt} \vec{r}_0 \cdot \vec{i}$$

where $\frac{d\mathfrak{R}(\theta_r, \theta_p, \theta_y)}{dt} \vec{r}_0$ determines the effect of the roll, pitch and yaw on Doppler shift of the scatterer at the location \vec{r}_0 .

When the target has perturbations in addition to its regular rotations, the conventional phase correction procedure is not suitable for correcting the additional phase errors, and the target may drift out from one range-Doppler cell into another. Thus, the ISAR image may become smeared.

A commercial small craft was used to study the effect of motion perturbation on ISAR images. The small craft data was collected by a X-band radar operating at 9.25GHz and transmitting a linear FM waveform with 500 MHz bandwidth or 0.3m range resolution. The coherent image integration time is 0.64s with 128 pulses. The roll, pitch and yaw rotations were obtained by on-board global positioning systems. These rotations can be used to investigate how the attitude and dynamics of the small craft can affect ISAR images.

From the corresponding GPS data, the actual roll, pitch and heading rotations are shown in Figure 6(c). Figure 6(a) shows a reconstructed clear image from one segment of the radar data. Figure 6(b) is the result from another data segment. The large perturbations of the roll, pitch and yaw angles cause image smearing. Image generated from the segment near 320,266 GPS-sec is smeared where large perturbations in the roll, pitch, and yaw angles can be seen. We can also see that image generated during the segment, where changes of the roll, pitch and yaw angles are relatively smaller, is a clear image. Thus, from the attitude measurements, we can estimate whether images can be reconstructed by using conventional algorithms.

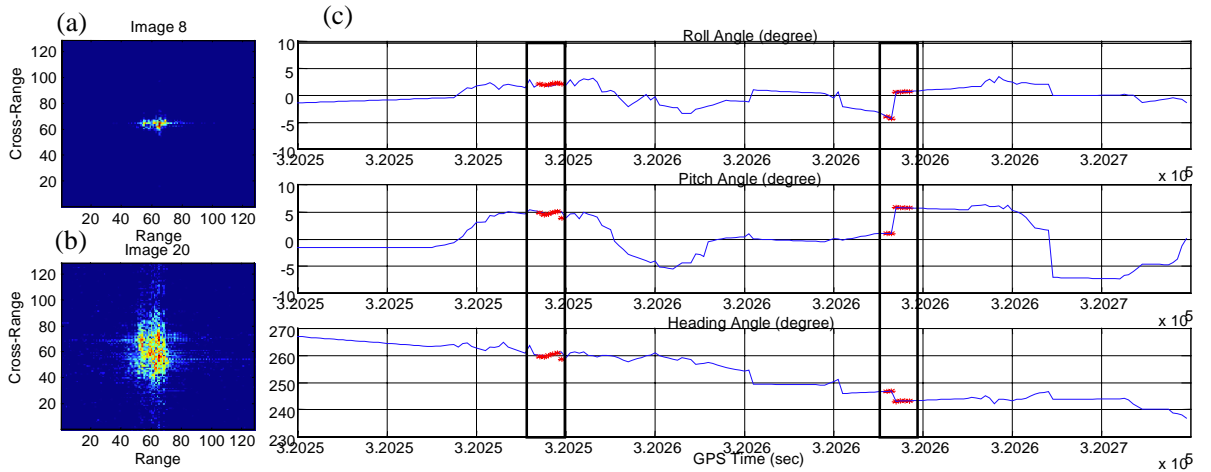


Figure 6. Effect of motion perturbation on ISAR images.

IV. SAR IMAGING OF GROUND MOVING TARGETS

SAR cannot simultaneously produce clear images of stationary targets as well as moving targets. Moving targets appear as defocused and spatially displaced objects superimposed on the SAR scene. In these cases, an important issue is the ability to detect and focus images of moving targets [13,15].

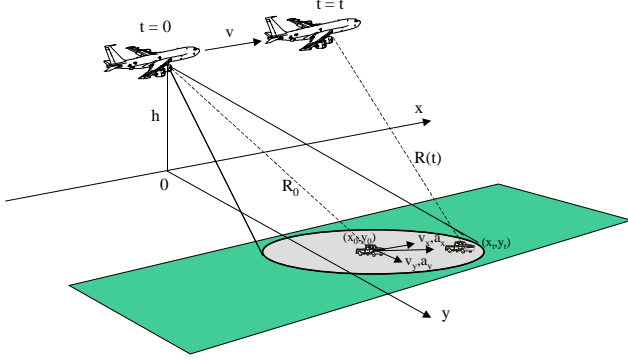


Figure 7. SAR imaging of ground moving targets.

A. The Effect of Target Motion on SAR Image

When the radar platform is moving along the azimuth direction at an altitude, and a point target at range R_0 is moving with a velocity v_y and an acceleration a_y in the radial direction, and a velocity v_x and an acceleration a_x in the azimuth direction as shown in Figure 7, then the Doppler shift of the returned signal consists of two parts: the part due to the radar motion

$$f_{D_{\text{Radar}}} = -\frac{2}{\lambda} \frac{x_0 v}{R_0} + \frac{2}{\lambda} \frac{v^2}{R_0} t$$

and the part due to the target motion

$$f_{D_{\text{Target}}} = -\frac{2}{\lambda} \frac{x_0 v_x + y_0 v_y}{R_0} + \frac{2}{\lambda} \frac{v_x^2 + v_y^2 + x_0 a_x + y_0 a_y - 2v v_x}{R_0} t$$

where the first term is the Doppler centroid and the second term is the Doppler rate induced by target motion.

Given a radar velocity v and an initial range from the radar to the target R_0 , the Doppler rate of the moving target is determined not only by its geometric location (x_0, y_0) but also by its velocity and acceleration. If the Doppler rate cannot be compensated, then the image of the moving target becomes defocused.

The quadratic phase variation between the target and the radar causes de-focusing of the moving target's image. When stationary objects are well focused, image of moving targets become de-focused and shifted in the cross-range direction.

To estimate the target's velocities and relocate mislocated moving targets, multiple-antenna (such as interferometry, planar apertures, or antenna array) approaches were proposed. Ground moving target indicator (GMTI) using multiple antennas has been proposed to reject radar returns from clutter and to detect moving target [13]. Single channel approach to GMTI was also studied [16].

B. Analysis of Ground Moving Target Data

Figure 8 shows a SAR image generated from X-band radar data without GMTI. We analyzed two small regions showing smeared structures along the cross-range direction. The region no.1 is located within range cells from no. 901 to no.964 and the region no.2 is from

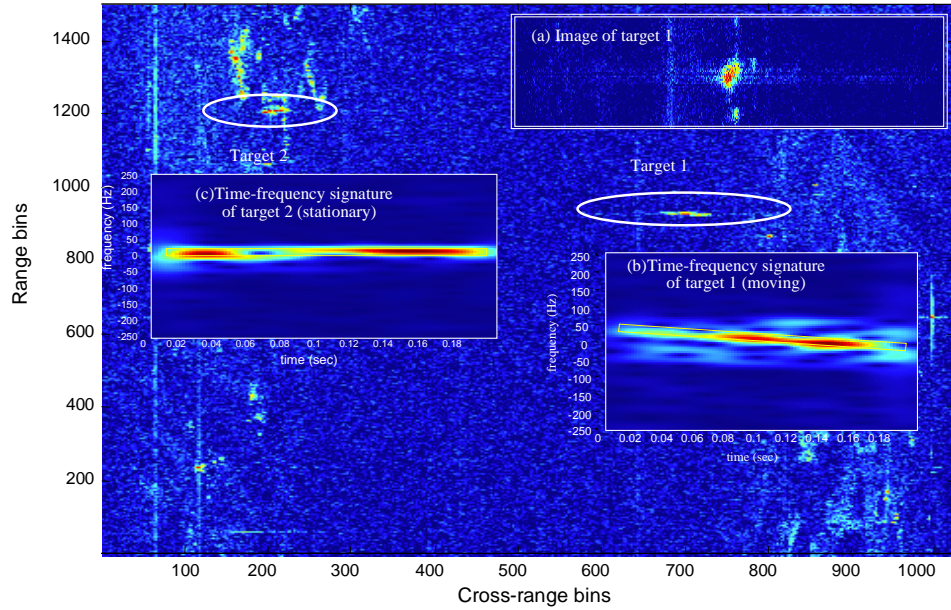


Figure 8. SAR images of ground moving targets.

no.1201 to no.1264. After focusing with phase correction, the image of the target in the region no.1 can be formed as in Figure 8(a). To further analyze the target, we take a small area around the target with 30 range cells and 100 cross-range cells. We analyze 100 pulses at range cell no.18, and the time-frequency signature is shown in Figure 8(b), where a ramped time-frequency signature indicates that the target is moving. For the region no.2, we have the time-frequency signature in Figure 8(c), where a flat time-frequency characteristic means the target is stationary. Time-frequency signatures can be used to distinguish moving targets from stationary targets and help in the detection of moving targets.

V. RADAR MICRO-DOPPLER FEATURE ANALYSIS

The micro-Doppler effect was originally introduced in coherent laser radar systems. In a coherent system, the phase of a signal returned from a target is sensitive to the variation in range. In many cases, a target or any structure on the target may have vibrations or rotations, called the micro-motion dynamics, in addition to its translation. The source of rotation or vibration may be a rotor of a helicopter, natural mechanical oscillations in a bridge or a building, an engine-induced vibrating surface, or other causes. The micro-motion dynamics produce frequency modulation on the backscattered signal and induce additional Doppler shifts to the Doppler frequency of the translation.

In microwave radar, micro-Doppler effect can also be observed. If the target is undergoing a vibration or rotation in addition to translations, then the Doppler frequency shift generated by the vibration or rotation is a time-varying frequency function and imposes a periodic, time-varying modulation onto the carrier frequency. Micro-Doppler can be regarded as a unique signature of the target and provides additional information that is complementary to existing methods [13,17].

To exploit these unique features of targets, traditional analysis, such as the Fourier transform or the sliding window FFT may not possess the necessary resolution for extracting these features. Therefore, high-resolution analysis is necessary for extracting micro-Doppler information.

The micro-Doppler frequency induced by rotations can be expressed as

$$f_{MicroDoppler} = \frac{2f}{c} [\vec{\omega} \times \vec{r}]_{radial}$$

where $\vec{\omega}$ is the rotation angular velocity and \vec{r} is the position vector of a point scatterer. We can see that the micro-Doppler of a point scatterer is usually a periodic frequency function of time.

A. Radar Micro-Doppler Feature of A Walking Man

Micro-Doppler effect of a walking person was also observed in radar reported in [17,18]. In [17], the radar

measurement data was collected by a rooftop X-band radar (data provided by Norden Systems, Northrop Grumman). A man walks towards a building at a speed of about 1.8 m/sec as illustrated in Figure 9(a).

The range profile has 64 range cells and the number of pulses is 1024 collected at a pulse repetition frequency of 800 Hz. Figure 9(b) shows a radar range-Doppler image of the walking man using 64 range-cells and 128 pulses, where the hot spot in the image indicates the body of the walking man. We also noticed that there are smeared lines running across the Doppler direction around the body of the walking man at the range cell no.12.

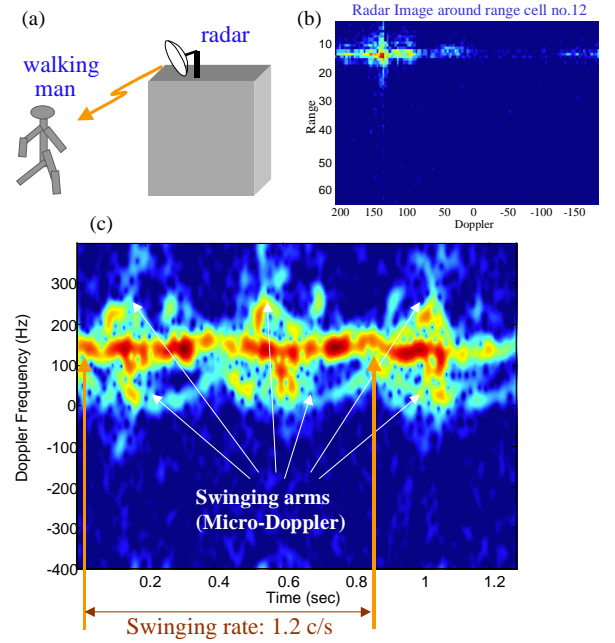


Figure 9. Radar micro-Doppler signature of a walking man.

By applying a time-frequency transform to the complex phase history data at range cell no.12, the body Doppler shift and the micro-Doppler shift of the swinging arms can be clearly detected in the joint time-frequency domain. The Doppler shift of one arm is higher and the other is lower than the body Doppler frequency shift. Superposition of time-frequency signatures over all range cells, which correspond to different walking steps, give a full time-frequency signature of the walking man as shown in Figure 9(c). We can see that the body's Doppler shift is almost constant but the arm's micro-Doppler shift is a time-varying periodic curve. From the available time information, the swinging rate of the arm can be estimated and is about 1.2 cycle/sec.

B. Radar Micro-Doppler Feature of Oscillating Corner Reflectors In SAR Scene

For SAR imaging, oscillating objects may cause phase modulation of the azimuth phase history data. The phase modulation can be seen as a time-dependent micro-Doppler frequency shift. Based on micro-Doppler signatures in the time-frequency domain, we can calculate the oscillating frequency and amplitude of oscillating corner reflectors in the SAR scene.

Figure 10(a) is a part of SAR scene taken by X-band SAR operating at 9.6 GHz and a pulse repetition frequency of 1,000 Hz. There are two corner reflectors shown in Figure 10(b) and located at range cell no.393 and no.400. Using the phase history data at the range cell no.393, by suppressing the ground clutter returns, the micro-Doppler signature of the oscillating corner reflector can be seen in Figure 10(c). It shows that the oscillation rate of the corner reflector is 2 Hz and the amplitude of the oscillation is 1.5 mm. The micro-Doppler signature of the phase history data at the range cell no.400 shown in Figure 10(d) indicates that the corner reflector at the range cell no. 400 is vibrating at multiple vibration rates.

IV. SUMMARY

In this paper, we reviewed advanced radar image formation and super-resolution, the effect of motion

perturbation on ISAR imaging, SAR imaging of ground moving targets, and radar micro-Doppler effect.

REFERENCES

- [1] Wehner, D.R., *High-Resolution Radar* (2nd ed.), Boston: Artech House, 1994.
- [2] Haywood, B. and Evans, R.J., "Motion Compensation for ISAR Imaging," Proceedings of Australian Symposium on Signal Processing and Applications, pp. 112-117, 1989.
- [3] Carrara, W.G., R.S. Goodman, and R.M. Majewski, *Spotlight Synthetic Aperture Radar – signal processing algorithms*, Artech House, Boston, 1995.
- [4] Lipps, R and Kerr, D. "Polar Reformatting for ISAR Imaging," Proceedings of the 1998 IEEE Radar Conference, pp.275-280, 1998.
- [5] Marple, S.L., *Modern Digital Spectral Estimation*, 1982.
- [6] Bottoms, M., R. Lipps and V.C. Chen, "ISAR Techniques for Target Identification", 2002 Combat Identification System Conference (CISC), vol. 1, 3-7, June, 2002.
- [7] Degraaf, S.R., "SAR imaging via modern 2-D spectral estimation methods", IEEE Trans. on IP, vol.7, no.5, pp.729-761, 1998.

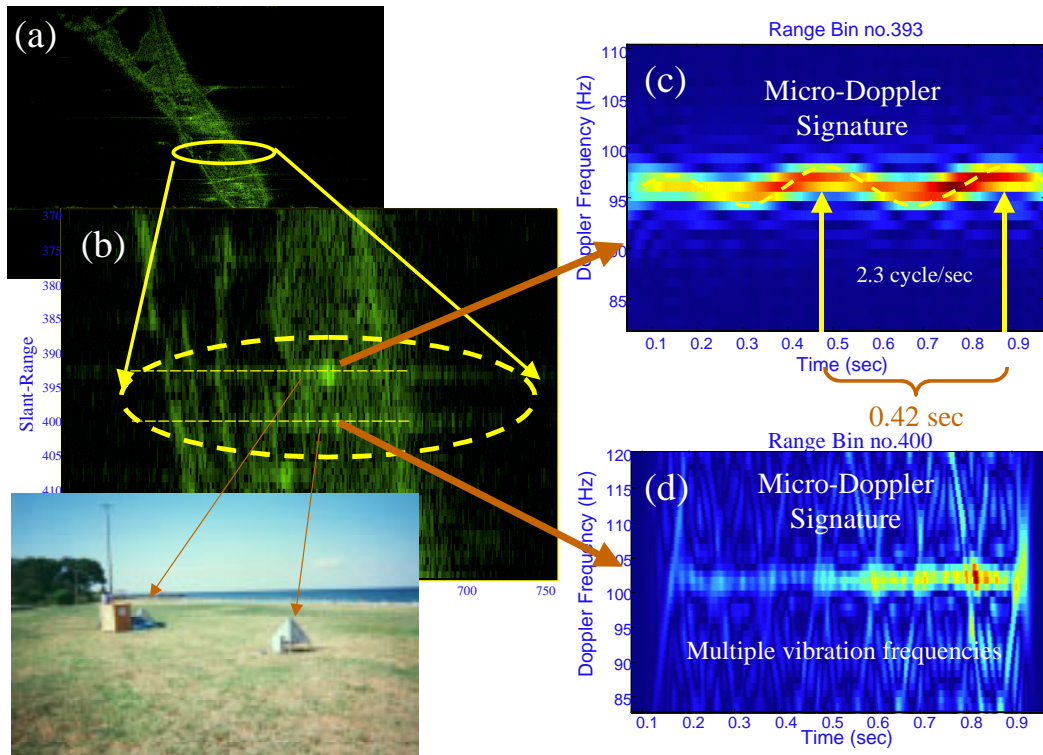


Figure 10. Radar micro-Doppler signature of corner reflectors.

- [8] Lam, L.K. and T.J. Abatzoglou, "Super resolution radar imagery based on 2D linear extension", 1993 Conference Record of The Twenty-Seventh Asilomar Conference on Signals, Systems and Computers, vol.1, pp.598–602, 1993.
- [9] Wu, R. and J. Li,, "Autofocus and super-resolution synthetic aperture radar image formation", IEE Proceedings - Radar, Sonar and Navigation, Vol. 147, no. 5, pp.217–223, 2000.
- [10] Pastina, D., A. Farina, J. Gunning, and P. Lombardo, "Two-dimensional super-resolution spectral analysis applied to SAR images", IEE Proceedings - Radar, Sonar and Navigation, , Vol. 145, no. 5, pp. 281 –290, 1998.
- [11] Chen, V.C. and S. Qian, "Joint Time-Frequency Transform for Radar Range-Doppler Imaging," IEEE Trans. on Aerospace and Electronic Systems, vol.34, no.2, pp.486-499, 1998.
- [12] Berizzi, F., E. Dalle Mese, M. Diani, and M. Martorella, "High-resolution ISAR imaging of maneuvering targets by means of the range instantaneous Doppler technique: modeling and performance analysis", IEEE Trans. on Image Processing, vol.10, no.2, pp.1880-1890, 2001.
- [13] Chen, V.C. and H. Ling, Time-Frequency Transforms for Radar Imaging and Signal Analysis, Artech House, Boston, 2002.
- [14] Chen, V.C., R. Lipps, "ISAR imaging of small craft with roll, pitch and yaw analysis", Proceedings of 2000 IEEE International Radar Conference, pp.493-498, 2000.
- [15] Chen, V.C., R. Lipps, and M. Bottoms, "Radar imaging of ground moving targets", Proceedings of the 2001 IEEE Radar Conference, pp.426-431, 2001.
- [16] Dias, J and P. Marques, "Multiple moving targets detection and trajectory estimation using a single SAR sensor", IEEE Trans. on AES, vol. 39, no.2, pp.604-624, 2003.
- [17] V. C. Chen, "Analysis of radar micro-Doppler signature with time-frequency transform", Proceedings of the IEEE Workshop on Statistical Signal and Array Processing (SSAP), Pocono, PA. pp.463-466, 2000.
- [18] Geisheimer, J.L., W.S. Marshall, and E. Greneker, "A continuous-wave (CW) radar for gait analysis", 35th Asilomar Conference on Signals, Systems and Computers, vol.1, pp.834-838, 2001.